J Mater Sci: Mater Med (2010) 21:2365–2369
DOI 10.1007/s10856-010-4090-9

Aqueous ferrofluids as templates for magnetic hydroxyapatite nanocomposites

Aparna Mir · Dhriti Mallik · Soumya Bhattacharyya · Dipankar Mahata · Arvind Sinha · Suprabha Nayar

Received: 15 January 2010 / Accepted: 26 April 2010 / Published online: 27 May 2010

Abstract Poly (vinyl) alcohol stabilized aqueous ferrofluids (PVA-ff) were used as nanotemplates for the crystallization of calcium hydroxyapatite (HAp). Four sets of PVA-ff-HAp nanocomposites were synthesized using 20, 40, 60 and 80 ml of PVA-ff for the same initial constituents of HAp. Various physico-chemical analyses suggest that the HAp lattice structure accommodates PVA-ff to a certain extent, beyond which the magnetic intra-molecular interactions predominate and PVA-ff starts to be pushed out of the HAp matrix. The in situ incorporation of PVA-ff during HAp synthesis results in a novel magnetic biomaterial with potential applications as targeted delivery vehicles.

1 Introduction

Hydroxyapatite (HAp) is similar to the main component of human bones and teeth, and it's compatibility with surrounding tissues is well known [1]. Nowadays, HAp-nanocomposites are used not only as bone graft substitutes, as carriers in targeted drug delivery systems but also for numerous engineering applications [2]. This paper describes the synthesis of a novel magnetic-hydroxyapatite nanocomposite. Superparamagnetic nanoparticles, which can be attracted to and maintained at a precise location by an external magnetic field, are being widely studied for use as targeted delivery vehicles [3]. If such magnetic nanoparticles can be incorporated into HAp, it will greatly enhance the specific delivery of drugs to the bone density deficit sites. In addition, the nano-iron oxide may act as an in vivo traceable agent. In order to achieve this, we have used poly (vinyl) alcohol (PVA) coated iron oxide in a fluid form as a template for the in situ synthesis of HAp to form a nanocomposite of iron oxide-HAp. The synthesized nanocomposites presumably have a core–shell structure. This new type of nanocomposite may prove to be a valuable candidate for tissue engineering applications, featuring a novel magnetic guiding option [4].

It is a well known fact that the physicochemical and biological properties of apatite accommodate different compositions and crystal structures [5–8]. The total iron pool of the body is composed of the iron in the red cell mass, tissue iron and a small amount of iron circulating in the plasma [9]. Thus, iron plays a vital role in the functioning of the body system. The utilization of magnetic iron oxide nanoparticles as a traceable agent has the added advantage that the toxicity of iron is masked to a great extent by its oxide form. Previous research has shown that iron ions are more toxic to the body than iron oxides at all concentrations [9–11]. Both HAp and aqueous PVA-ff have a number of reported biomedical applications separately [12–14], but a combination of the two has not been adequately explored. Reports suggest that Fe(III) ions with high spin substitute into the apatite structure and Fe-HAp with a pure apatitic phase is obtained [15]. While some research has been carried out to impart ferromagnetic properties to bone cement [16], we have been successful in imparting superparamagnetic properties to the nanocomposite at ambient conditions.

A. Mir · D. Mallik (✉) · S. Bhattacharyya · A. Sinha · S. Nayar
National Metallurgical Laboratory, Jamshedpur 831007, India
e-mail: dhritimallik@nmlindia.org

D. Mahata
Burdwan University, Burdwan, India

2 Materials and methods

2.1 Materials

All the chemicals used were of analytical grade. Ferric chloride ($FeCl_3 \cdot 6H_2O$), ferrous chloride were purchased from Rankem, poly (vinyl) alcohol (mol wt. 44,000) (PVA) from Qualigenes, Di-ammonium hydrogen phosphate and ammonia solution (30%) from Merck and calcium nitrate $Ca(NO_3)_2 \cdot 4H_2O$ from Himedia.

2.2 Experimental procedure

To prepare PVA-ff-HAp nanocomposites, the wet co-precipitation method has been used.

$$10\ Ca(NO_3)_2.\ 4H_2O + 6(NH_4)_2HPO_4 + 8\ NH_4OH \rightarrow Ca_{10}(PO_4)_6(OH)_2 + 46\ H_2O + 20\ NH_4NO_3$$

Alkaline calcium nitrate solution containing 0.5% PVA was made, to which different volumes of aqueous PVA-ff (20, 40, 60, 80 ml respectively) were added. After incubating for 24 h, alkaline di-ammonium hydrogen phosphate was added for precipitation of HAp. The pH of the slurry was maintained at 10.5. The sample was then aged for a time period of 7 days after which the slurry was washed till pH 7 and oven dried. The powder thus obtained, was structurally and magnetically characterized.

3 Characterization

3.1 X-ray diffraction (XRD)

The crystal structure of the nanocomposites were characterized using XRD (Siemens D500) within a 2θ range of 20°–80° by Cu Kα ($\lambda = 1.54$ angstrom) radiation.

3.2 Transmission electron microscopy (TEM)

The size, morphology of the synthesized PVA-ff-HAp nanocomposites were determined using transmission electron microscope (TEM) (CM 200, CXPhilips at 160 kV).

3.3 Fourier transform infrared spectroscopy (FTIR)

Fourier Transform Infrared Spectroscopy (NICOLET-759) was used to check the functional groups of the PVA-ff-HAp powder. Scans between the wavelengths 4000 and 400 cm^{-1} were recorded using potassium bromide pellet method.

3.4 Vibrating sample magnetometry (VSM)

The magnetic properties were studied using Vibrating Sample Magnetometer (VSM LAKE SHORE-7040) in an applied field range of ±1.5 Tesla at room temperature.

4 Results

4.1 X-ray diffraction (XRD) studies

The XRD of PVA-ff shows peaks corresponding to those of magnetite and maghemite, the prominent ones being (220), (311), (400), (422), (511) and (411). On addition of 20, 40, 60 and 80 ml volume of PVA-ff to in situ HAp synthesis machinery, the iron oxide peaks get masked and only the predominant HAp peaks are revealed (211), (300), (002), (024), (222) and (202). The HAp lattice seems to be intact and iron oxide may be getting accommodated in the interstitial spaces (Fig. 1).

4.2 Transmission electron microscopy (TEM)

The pure PVA-ff micrograph shows typical cuboidal nanoparticles of iron oxide in a necklace like arrangement. In the PVA-ff-HAp nanocomposites using 20 and 40 ml PVA-ff, the necklace arrangement seems to get compacted because of the nucleation of acicular shaped HAp crystals on it. There seems to be a tendency of the necklace arrangement to straighten out in order to allow nucleation of HAp [17]. Since the reagents for HAp nucleation are same in all the three samples, in the PVA-ff-HAp (60 ml) nanocomposite, we see the beginning of a phase separation of PVA-ff, not observed in the other samples. It could be a case of PVA-ff templated HAp self-assembly because of

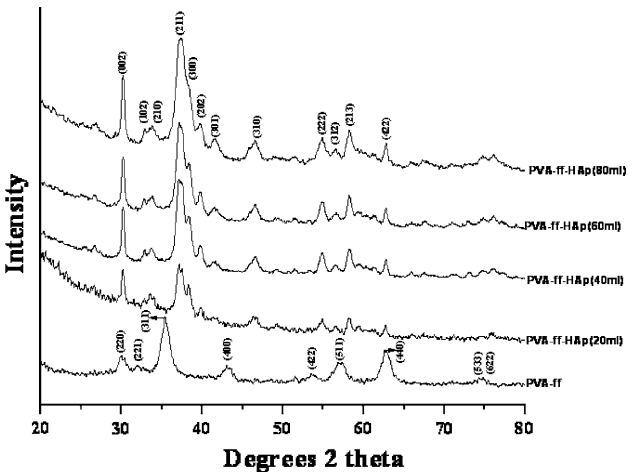

Fig. 1 Comparative XRD data of pure PVA-ff and the PVA-ff-HAp nanocomposites

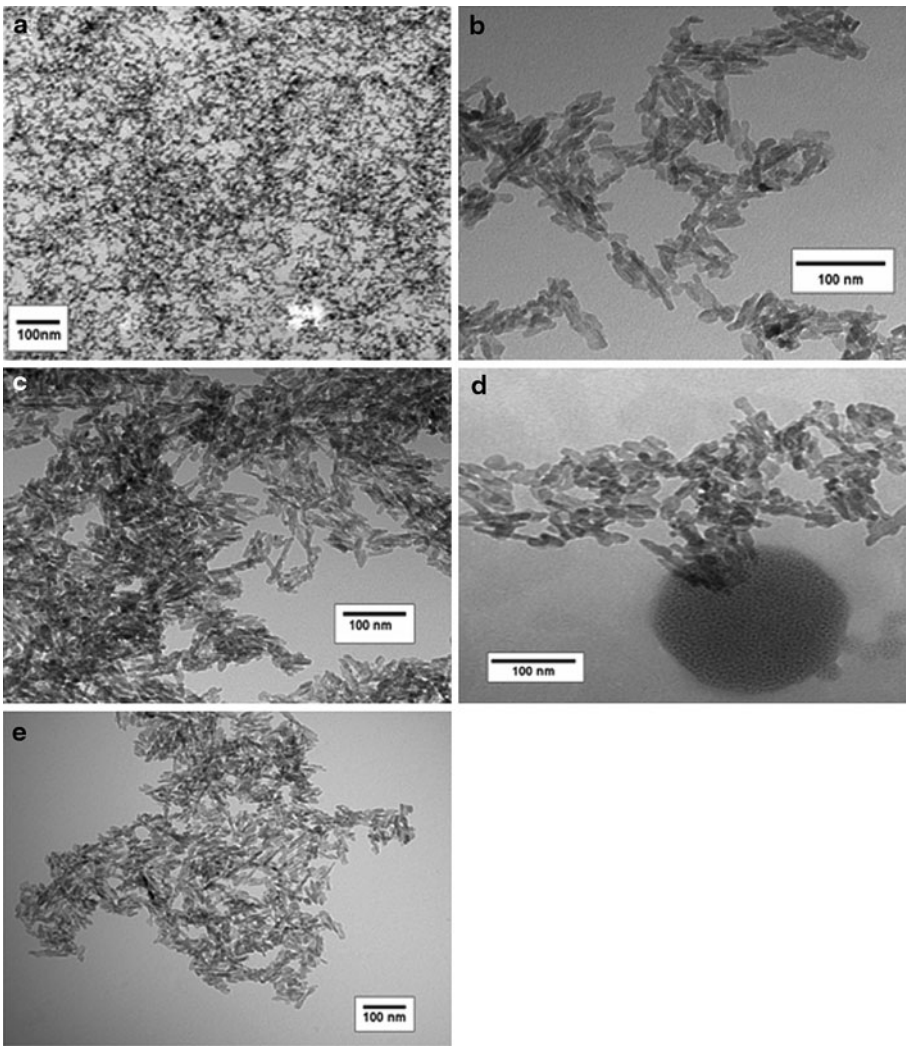

Fig. 2 TEM images showing (**a**) necklace like arrangement of pure PVA-ff (**b**–**e**) arrangement of PVA-ff-HAp nanocomposites containing 20, 40, 60 and 80 ml of PVA-ff respectively

magnetic interactions, the resulting spatial/steric interactions cause the iron oxide, to which HAp is not associated, to agglomerate separately (Fig. 2). It is noteworthy that the particle size of the iron oxide in PVA-ff has an average size of 5 nm and the HAp crystals are about 20 nm in all the nanocomposites. The increasing volume of PVA-ff seems to magnetically compact the overall system.

4.3 Fourier transform infrared spectroscopy (FTIR)

The −OH stretching and bending positions have shown considerable change in the nanocomposites suggesting a strong interaction between groups of the synthesized PVA-ff-HAp nanocomposites. The −OH stretching band of pure PVA at 3466 cm^{-1} has red-shifted to 3436 cm^{-1} in the nanocomposite and the −OH bending band at 1654 cm^{-1} of pure PVA has red-shifted to 1640 cm^{-1} along with a peak broadening and a substantial increase in transmittance intensity. The presence of the C–H stretching band at 2924 cm^{-1} is observed in the 20, 40, 60 and 80 ml samples which is characteristic of HAp. There is a remarkable change in the insignificant peak of −CH bending band at 1403 cm^{-1} of PVA-ff. The interaction between the PVA-ff and HAp seems to have brought about a conformational change that has caused a major blue-shift to 1440 cm^{-1}. Intermolecular hydrogen bonding may also have occurred among PVA chains due to the hydroxyl groups [18]. The bands at 1120 and 910 cm^{-1} of –C–O–C and −C = C of pure PVA becomes more intense and forms a predominant one at 1040 cm^{-1}. Iron oxide bands appear at 540, 570 and 630 cm^{-1} for hematite, magnetite and maghemite respectively [19]. For the nanocomposites synthesized here, the value is 565 cm^{-1} for 20, 40, and 60 ml and 577 cm^{-1} for 80 ml, are closest to magnetite. It is well established that nano-magnetite has no strong IR bands in the frequency region above 650 cm^{-1} [20]. From the FTIR features, it is evident that there are strong chemical interactions between PVA-ff and the nucleating HAp nanoparticles (Fig. 3).

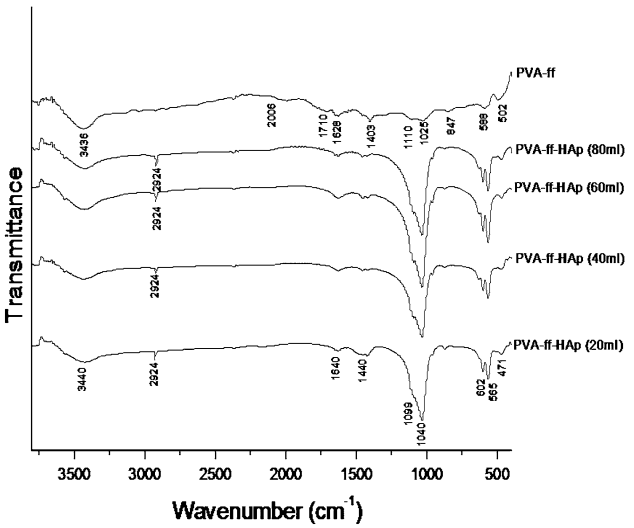

Fig. 3 FTIR curves of PVA-ff and PVA-ff-HAp nanocomposites

4.4 Vibrating sample magnetometry (VSM)

The expectation from magnetization studies (Fig. 4) was that as the volume of PVA-ff increases, the iron content increases, and so would the saturation magnetization, but, the following values of magnetization: 1.3406, 2.6746, 2.4739, 3.4082 A.m^2/kg for 20, 40, 60 and 80 ml PVA-ff were obtained. A decrease in M_s denotes a decrease in magnetic moment per unit volume and the above surprising values may be explained based on core–shell interactions. As HAp concentration remains unchanged in all the samples (HAp is a universal adsorbent and hence may serve as a coating material), the PVA-ff-HAp (20 ml) sample has a small core size; as we increase the PVA-ff volume, the magnetic interaction increases and thus the core increases and there is an increased interaction between the core and HAp. This masks the magnetic moment to some extent in the PVA-ff-HAp (40 ml) sample and greatly in the nanocomposites containing 60 ml PVA-ff. In the PVA-ff-HAp (80 ml) sample, a positive enhancement in magnetization is observed because of the free PVA-ff, which is not part of HAp nucleation and hence not adsorbed by HAp. 60 ml PVA-ff seems to be the limiting factor in the PVA-ff-HAp nanocomposite, as seen by the coercivity values of PVA-ff-HAp (80 ml) which is 18.43 G, very close to that of free PVA-ff, which is 19.641G. PVA-ff-HAp (20 ml) has the maximum coercivity of 48.046G-which could be due to the increase in the core size with HAp formation. Coercivity, however, further decreases with increasing PVA-ff. The coercivity values of PVA-ff-HAp (40 ml) being 34.696G and PVA-ff-HAp (60 ml) being 24.356 G proves that increasing PVA-ff in the presence of HAp restricts an increase in core-size.

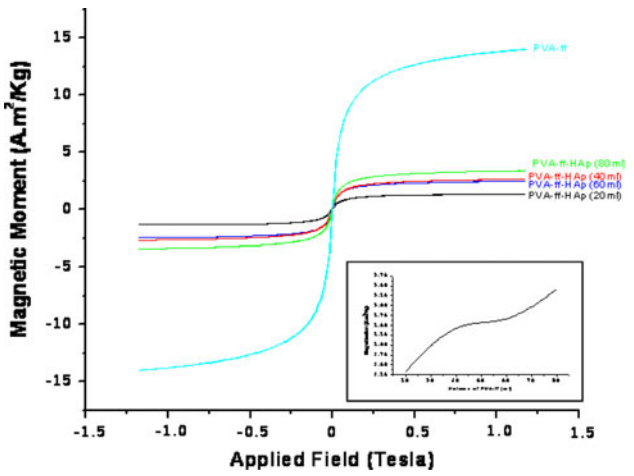

Fig. 4 Magnetization studies of the four nanocomposites and pure PVA-ff. Inset showing variation in saturation magnetization with increasing PVA-ff concentration

5 Conclusion

The association of in situ synthesized HAp particles with PVA-ff is difficult to classify whether it is adsorption, diffusion, or chemical bond formation. TEM micrographs reveal the nanosize of the synthesized composites while the XRD pattern predicts the incorporation of the iron oxide nanoparticles in the interstitial spaces of HAp without disrupting its lattice structure. FTIR results suggest the presence of either covalent or numerous hydrogen/Van der Waals interactions between the components of the nanocomposite while VSM studies prove its superparamagnetic property. In spite of its important role in living systems, nanosized iron is known to be toxic to cells and it is necessary to sequester it in a non-toxic form. This PVA-ff-HAp nanocomposite could hence prove to be a useful biomaterial once we establish its biocompatibility studies.

References

1. Glimcher MJ. Molecular biology of mineralized tissues with particular reference to bone. Rev Mod Phys. 1959;31:359–93.
2. Nakahira A, Nakamura S, Horimoto M. Synthesis of modified hydroxyapatite (HAp) substituted with Fe ion for DDS application. IEEE Trans Mag. 2007;43:2465–7.
3. Wu HC, Wang T, Bohn MC, Lin F, Spector M. Novel magnetic hydroxyapatite nanoparticles as non-viral vectors for the glial cell line-derived neurotrophic factor gene. Adv Func Mater. 2010;20:67–77.
4. Bock N, Riminucci A, Dionigi C, Russo A, Tampieri A, Landi E, Goranov VA, Marcacci M, Dediu V. A novel route in bone tissue engineering: magnetic biomimetic scaffolds. Acta Biomater. 2010;6:786–96.

5. Kumta PN, Sfeir C, Lee DH, Olton D, Choi D. Nanostructured calcium phosphates for biomedical applications: novel synthesis and characterization. Acta Biomater. 2005;1:65–83.
6. Matsumoto T, Okazaki M, Inoue M, Yamaguchi S, Kusunose T, Toyonaga T, Hamada Y, Takahashi J. Hydroxyapatite particles as a controlled release carrier of protein. Biomaterials. 2004;25: 2807–12.
7. Mizushima Y, Ikoma T, Tanaka J, Hoshi K, Ishihara T, Ogawa Y, Ueno A. Injectable porous hydroxyapatite microparticles as a new carrier for protein and lipophilic drugs. J Control Release. 2006;110:260–5.
8. Morrissey R, Rodriguez-Lorenzo LM, Gross KA. Influence of ferrous iron incorporation on the structure of hydroxyapatite. J Mater Sci Mater Med. 2005;16:387–92.
9. Yamasaki K, Hagiwara H. Excess iron inhibits osteoblast metabolism. Toxicol Lett. 2009;191:211–5.
10. Berry CC. Possible exploitation of magnetic nanoparticle–cell interaction for biomedical applications. J Mater Chem. 2005;15: 543–7.
11. Dobson J. Nanoscale biogenic iron oxides and neurodegenerative disease. FEBS Lett. 2001;496:1–5.
12. Webster TJ, Massa-Schlueter EA, Smith JL, Slamovich EB. Osteoblast response to hydroxyapatite doped with divalent and trivalent cations. Biomaterials. 2004;25:2111–21.
13. Nazarpak MH, Solati-Hashjin M, Moztarzadeh F. Preparation of hydroxyapatite ceramics for biomedical applications. J Ceram Proc Res. 2009;10:54–7.
14. Ito A, Shinkai M, Honda H, Kobayashi T. Medical application of functionalized magnetic nanoparticles. J Biosci Bioeng. 2005;100:1–11.
15. Wang J, Toru N, Kunio Y. Syntheses, structures and photophysical properties of iron containing hydroxyapatite prepared by a modified pseudo-body solution. J Mater Sci Mater Med. 2008;19:2663–7.
16. Gross KA, Jackson R, Cashion JD, Rodriguez-Lorenzo LM. Iron substituted apatites: a resorbable biomaterial with potential magnetic properties. Euro Cell Mater. 2002;3:114–7.
17. Guha AK, Singh S, Kumaresan R, Nayar S, Sinha A. Mesenchymal cell response to nanosized biphasic calcium phosphate composites. Coll Surf B Bioint. 2009;73:146–51.
18. Mansur HS, Sadahira CM, Souza AN, Mansur AAP. FTIR spectroscopy characterization of poly (vinyl alcohol) hydrogel with different hydrolysis degree and chemically crosslinked with glutaraldehyde. Mater Sci Eng C. 2008;28:539–48.
19. Nasrazadani SH. Quantitative analysis of iron oxides using Fourier transform infrared spectrophotometry. Corr Sci. 2008;50: 2493–7.
20. Marinescu G, Patron L, Culita DC, Neagoe C, Lepadatu CI, Balint I, Bessais L, Cizmas CB. Synthesis of magnetite nanoparticles in the presence of aminoacids. J Nano Res. 2006;8: 1045–51.